Temperature Trapping: Energy-Free Maintenance of Constant Temperatures as Ambient Temperature Gradients Change

Xiangying Shen,[1,3] Ying Li,[2] Chaoran Jiang,[1,3] and Jiping Huang[1,3,*]
[1]Department of Physics, State Key Laboratory of Surface Physics, and Key Laboratory of Micro and Nano Photonic Structures (MOE), Fudan University, Shanghai 200433, China
[2]Department of Mechanics and Engineering Science, Fudan University, Shanghai 200433, China
[3]Collaborative Innovation Center of Advanced Microstructures, Nanjing 210093, China
(Received 31 March 2016; published 29 July 2016)

It is crucial to maintain constant temperatures in an energy-efficient way. Here we establish a temperature-trapping theory for asymmetric phase-transition materials with thermally responsive thermal conductivities. Then we theoretically introduce and experimentally demonstrate a concept of an energy-free thermostat within ambient temperature gradients. The thermostat is capable of self-maintaining a desired constant temperature without the need of consuming energy even though the environmental temperature gradient varies in a large range. As a model application of the concept, we design and show a different type of thermal cloak that has a constant temperature inside its central region in spite of the changing ambient temperature gradient, which is in sharp contrast to all the existing thermal cloaks. This work has relevance to energy-saving heat preservation, and it provides guidance both for manipulating heat flow without energy consumption and for designing new metamaterials with temperature-responsive or field-responsive parameters in many disciplines such as thermotics, optics, electromagnetics, acoustics, mechanics, electrics, and magnetism.

DOI: 10.1103/PhysRevLett.117.055501

It is known that humans are faced with a global energy crisis, namely, an increasing shortage of nonrenewable energy resources, such as coal, petroleum, and natural gas [1]. However, much of the energy generated from nonrenewable energy resources is used for temperature preservation in many areas ranging from industrial fields to our daily lives. Therefore, it is meaningful and challenging to reduce such energy consumption.

Heat conduction exists in matter as long as there is a temperature gradient. In recent years, researchers have been devoted to understanding and controlling the conduction of heat, putting a particular emphasis on its nonlinear feature. Their fundamental interests focus on the nonlinear conduction phenomenon at the microscopic scale to have a better understanding [2,3], to improve thermoelectric effects [4–6], or to achieve novel thermal rectification [7–9]. However, the nonlinear heat conduction at the macroscopic scale is seldom touched in the field of fundamental research even though it was already reported long ago [10]. In this work, by tailoring the nonlinear effect of macroscopic heat conduction [10,11], namely, manipulating thermally responsive thermal conductivities appropriately, we establish a temperature-trapping theory and then propose a novel concept of an energy-free thermostat. The thermostat can self-maintain a desired constant temperature without the need of consuming energy even though the environmental temperature gradient changes in a large range. As a proof of concept, we experimentally fabricate a prototype device by assembling commercially available materials according to a multistep approximation method, which enables us to effectively realize the desired thermal conductivities on the same footing as thermal metamaterials [11–18] or metamaterials in other fields [19–22]. Then we apply the thermostat concept to thermal cloaking [11–18] as a model application, and show an improved thermal cloak, whose central region serves as an ideal thermal environment with a constant temperature even though the environmental temperature gradient varies significantly. This feature makes the improved thermal cloak distinctly different from the existing thermal cloaks [11–18].

Temperature-trapping theory: Concept of energy-free thermostat.— It is known that thermal conductivities essentially depend on temperature, T [10]. Particularly, in a phase transition process, the thermal conductivity can change sharply [23]. For simplicity, let us consider a one-dimensional steady-state heat conduction along the x direction with temperature-dependent thermal conductivities, $\kappa(x,T)$. The conduction follows the differential equation,

$$\frac{d}{dx}\left(\kappa(x,T)\frac{dT}{dx}\right)=\frac{\partial\kappa(x,T)}{\partial x}\frac{dT}{dx}+\frac{\partial\kappa(x,T)}{\partial T}\left(\frac{dT}{dx}\right)^2+\kappa(x,T)\frac{d^2T}{dx^2}=0. \quad (1)$$

Then we are in a position to find a specific value or function of $\kappa(x,T)$ for our purpose: the temperature at a specific region should keep (almost) unchanged even though the associated boundary conditions change significantly. In other words, we expect that the desired material

should be able to automatically maintain a constant temperature within changing ambient temperature gradients without the need of adding additional work.

For more details, let us consider the one-dimensional model, where the right-hand (left-hand) side of the model is the heat (cold) source with a fixed high (low) temperature of T_H (T_L). We set T_c as an arbitrary value between T_H and T_L. As T_H increases (or T_L decreases), we expect that the temperature at the middle point (located between the hot and cold sources) should always be T_c. Now, suppose the model is divided into two parts from the middle point: the temperature of part I ranging from T_H to T_c, and part II from T_c to T_L. In case of increasing T_H only, for any $\kappa(x,T)$, the temperature in part II should always range from T_c to T_L. Therefore, in part II, the temperature gradient remains unchanged, yielding a corresponding heat flow. Since T_H may increase and it has no effect on the temperature at the middle point, the heat flow must be independent of T_H. Owing to the continuity of heat flow, we obtain

$$q = -\kappa(x,T)\frac{dT}{dx} \equiv C, \tag{2}$$

where q is the density of heat flow, and C is a constant. Clearly, if only considering a decreasing T_L, we may obtain the same equation as Eq. (2). This fact means that our models are centrosymmetric: $\kappa(x,T)$ are symmetrical with respect to $T = T_c$. Equation (2) is the key for giving a rough sketch of

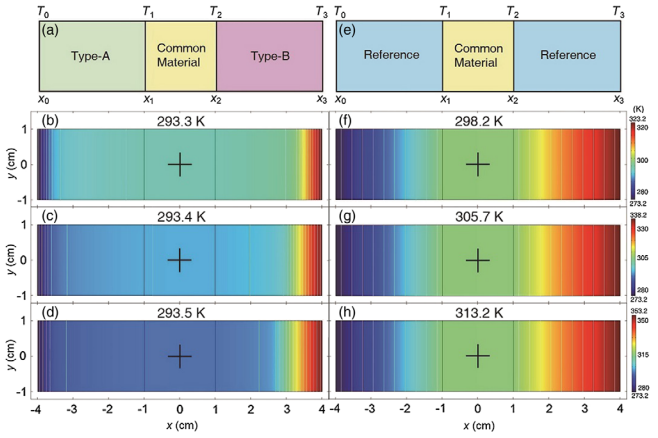

FIG. 1. (a) Schematic graph showing the design of an energy-free thermostat, which consists of three parts: common material (2 cm width and 2 cm height), type-A and type-B nonlinear materials (each with 3 cm width and 2 cm height). (b)–(d) Finite-element simulations of (a) according to Eq. (3) where $\delta = 0.4$ W/m · K, $\varepsilon = 49.6$ W/m · K, and $T_c = 293.2$ K. (e) Schematic diagram of a reference model. (f)–(h) Finite-element simulations of (e), where the thermal conductivity of the reference material [denoted by blue in (e)] is 50 W/m · K. For all the simulations (b)–(d),(f)–(h), the temperature at the center (marked with +) is extracted and shown above each panel. The thermal conductivity of the central common material is 400 W/m · K. The left boundary is kept at a constant low temperature, 273.2 K, while the right boundary is kept at different high temperatures: 323.2 (b),(f), 338.2 (c),(g), and 353.2 K (d), (h). The upper and lower boundaries are thermally insulated.

$\kappa(x,T)$. As $T \to T_c$, $dT/dx \to 0$. Thus, $\kappa(x,T)$ should tend to infinity and reach the highest value. On the contrary, for $T \gg T_c$ or $T \ll T_c$, the temperature gradients are large, so $\kappa(x,T)$ tends to zero. Moreover, the middle point with $T = T_c$ is the inflection point of function $\kappa(x,T)$. To sum up, the temperature-dependent function, $\kappa(x,T)$, should satisfy the following rules: $\kappa(x,T-T_c) = \kappa(x,T_c-T)$; $\kappa(x,T) \to \infty$ as $T \to T_c$; and $\kappa(x,T) \to 0$ as $T \gg T_c$ or $T \ll T_c$. The second requirement is not realistic for extant materials and some approximation should be adopted instead.

In consideration of mathematical simplicity for easy analysis and modeling, we design an alternative one-dimensional heat conduction model as shown in Fig. 1(a), where T_3, T_2, T_1, and T_0 (or x_3, x_2, x_1, and x_0) are the corresponding temperatures (or positions) along the direction of heat diffusion, where we set $x_1 - x_0 = x_3 - x_2$. Two types of nonlinear materials (type A and type B) are located at the left-hand and right-hand sides, respectively, and a common material with a high and constant conductivity κ_η is placed in the middle region. In this model, the conductivities of type A and B are related to the temperature, and the relations are chosen to hold the same form as the logistic functions $L(T)$ widely used in logistic regressions. We believe the combination of a pair of axial symmetry logistic functions may give a good approximation of the aforementioned requirements of thermal conductivity. Furthermore, these two types of materials are much more practicable because the sigmoid curves indicated by logistic functions are similar to those "S" shape curves in phase transition materials describing physical properties as a function of temperature [23–25].

More explicitly, the type-A nonlinear material is designed with thermal conductivity κ_A as a conductor (or an insulator) at high (or low) temperature. An inverse behavior happens for the type-B material with thermal conductivity κ_B. For a given phase-transition temperature T_c, both κ_A and κ_B may be assumed as

$$\kappa_A = L(T_c - T) = \delta + \frac{\varepsilon e^{T-T_c}}{1+e^{T-T_c}},$$
$$\kappa_B = L(T - T_c) = \delta + \frac{\varepsilon}{1+e^{T-T_c}}, \tag{3}$$

where δ is a small value and ε is high enough. In Eq. (3), $T - T_c$ has a prefactor, $1K^{-1}$, which has been omitted throughout this work. According to the Fourier law $q = -\kappa(dT/dx)$ or $qdx = -\kappa dT$ together with the geometrical relation ($x_1 - x_0 = x_3 - x_2$) and continuity of conduction $\int_{x_0}^{x_1} qdx = \int_{x_2}^{x_3} qdx$ or $\int_{T_0}^{T_1} \kappa_A dT = \int_{T_2}^{T_3} \kappa_B dT$, we obtain (under the assumption that $e^{T_0-T_c}$ and $e^{T_c-T_3}$ are close to zero),

$$(\varepsilon+\delta)(T_3 - T_2) - \varepsilon(T_3 - T_c) - \delta(T_1 - T_0)$$
$$= \varepsilon \ln\left(\frac{1+e^{T_1-T_c}}{1+e^{T_2-T_c}}\right). \tag{4}$$

It should be remarked that the thermal conductivity in the middle region should be much higher ($\kappa_\eta \gg \varepsilon$) to make $T_1 \approx T_2$. As a result, the relation $T_1 \approx T_2 \approx T_c$ can be

obtained according to Eq. (4). Therefore, the temperature preserved in our device is approximately the phase-transition temperature, T_c. The above discussion shows that adopting two Logistic functions is enough for energy-freely maintaining constant temperatures as ambient temperature gradients change.

Then we perform finite-element simulations according to Eq. (3). In Fig. 1, the central temperatures at the positions marked with a + show a strong contrast between the thermostat [Figs. 1(b)–1(d)] and the reference system [Figs. 1(f)–1(h)]. The former are close to T_c (within 0.3 K) for the three cases. On the contrary, the latter deviate from T_c as far as 20 K when the boundary condition changes within the same range. It is worth noting that the temperature of the cold source in Figs. 1(b)–1(d), 1(f)–1(h) remains constant (273.2 K) for the sake of comparison. Actually, if this temperature varies as well, the behavior of the central temperatures will keep unchanged due to the fixed value of T_c.

Experimental demonstration of the energy-free thermostat concept.— The major challenge in realizing the thermostat is to find the type-A and type-B materials with nonlinear (temperature-dependent) conductivities [Eq. (3)]. Although phase transitions may generate such variations of conductivities, the transition process is not convenient in operations. We believe that a simplest temperature-dependent conductivity is to switch between two values, which can be achieved by connecting two thermal conductors or not. This process may be described by a step function. To make the conductivity vary as a step function, a practical way is to assemble a still part and a movable part. Figure 2 shows the relevant details.

In our experiment, the still part is constructed by placing three phosphor copper (QSn6.5-0.1) films ($\kappa_p = 54\ \mathrm{W/m \cdot K}$) at regular intervals; each interval is filled with silicon grease ($\kappa_s = 4\ \mathrm{W/m \cdot K}$). All the phosphor copper films and their intervals (filled with silicon grease) hold the same dimensions. As a result, the effective thermal conductivity of this alternating layered structure can be derived as $\kappa_{\mathrm{eff}} = [(\kappa_p^{-1} + \kappa_s^{-1})/2]^{-1} = 7.4\ \mathrm{W/m \cdot K}$ [26]. On the other hand, a bimetallic strip composed of phosphor copper and shape memory alloy (SMA) [27,28] serves as the movable part.

The SMA is capable of changing its shape as the temperature varies. Specifically, a two-way SMA chosen for building the type-A material is able to tilt up an angle below 278.2 K and completely level above 297.2 K. For the type-B material, the transition temperatures are the same but the deformation is opposite. Therefore, as we change the temperature of the hot or cold source, the bimetallic strips will be driven up and down. In general, due to the deformation of SMA, 0–3 metal films will fill the gaps between the two connective layers of phosphor copper [Figs. 2(a)–2(b)], and change the effective conductivity of type-A or type-B material according to the effective medium theory [26]. The calculated thermal conductivities are displayed in Fig. 2(c). It should also be noted that the

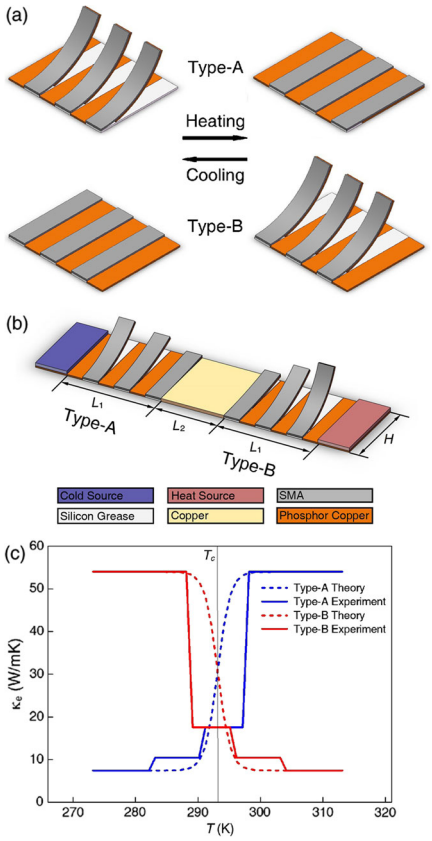

FIG. 2. (a) Schematic graph showing the type-A and type-B nonlinear materials of the energy-free thermostat fabricated in our experiment. For the type-A part, the bimetallic strips will tilt up and result in a low effective thermal conductivity κ_{eff} of the layered structure when the temperature is below 297.2 K. Upon heating, the bimetallic strips will become level and replace the silicon grease layers with phosphor copper when the temperature is above 297.2 K. As a result, κ_{eff} increases. The opposite behavior happens for the deformation of the type-B part. When a temperature gradient exists in the device, the bimetallic strips show different degrees of deformation; see (b). The dimensions indicated in (b): $L_1 = 3$, $L_2 = 2$, and $H = 2$ cm. Since κ_{eff} of the type-A or type-B part depends on the shapes of the bimetallic strips, which vary with the temperature T_S of the heat or cold sources, we can achieve a relationship $\kappa_{\mathrm{eff}}(T_S)$ that is similar to $\kappa_A(T)$ or $\kappa_B(T)$ in Eq. (3). This similarity serves as the main principle of our experiment; see (c). The solid curves indicated by "Experiment" are calculated with the effective medium theory by assuming the leveling of 0–3 bimetallic strips; the dashed curves indicated by "Theory" are the result of Eq. (3).

transition temperature T_c of the type-A and type-B materials are actually 297.2 K, since at this temperature, the three SMAs are all flat (or warped) for type-A (or type-B).

In addition, a copper film with $\kappa_\eta = 394\ \mathrm{W/m \cdot K}$ is located in the middle to assemble the whole device; see Fig. 2(b). Moreover, all the metal surfaces are covered by polydimethylsiloxane, which helps against heat dissipation and makes the whole device "visible" for the thermal camera.

As shown in Fig. 3, the experiment is carried out for three different boundary conditions, where the temperature of the

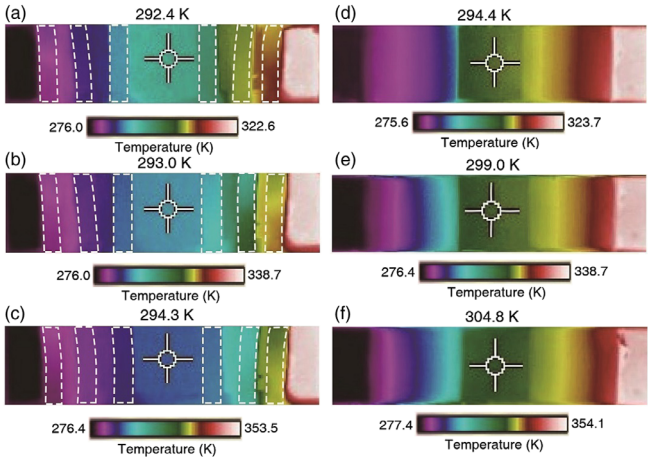

FIG. 3. Experimental results. The temperature at each center is displayed above the corresponding panel. For the energy-free thermostat (a-c), the bimetallic strips are indicated with white dashed lines. As the temperature of the heat source varies in a wide range (322.6–353.5 K), the central temperature keeps almost unchanged (a-c). In contrast, for the reference system (d-f), the measured central temperature varies evidently.

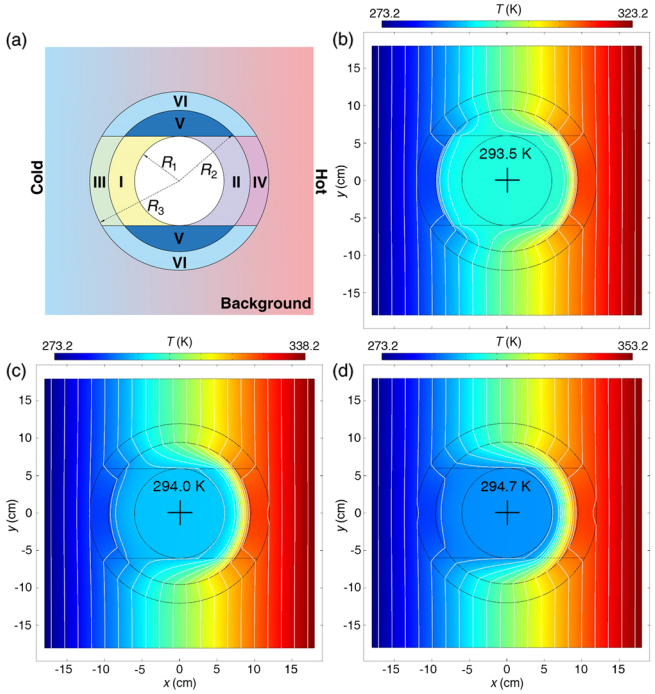

FIG. 4. (a) Schematic graph showing the improved bilayer thermal cloak in a background. The thermal conductivities in regions I-IV (or V-VI) are determined by Eq. (5) [or Eq. (6)]. (b)–(d) Finite-element simulations of the improved thermal cloak, where the white lines denote the isothermal lines. (b)–(d) Show a central circular region where the temperature keeps approximately unchanged even though the temperature of the heat source increases significantly. Parameters: $\kappa_0 = 2.3$ W/m · K, $\kappa_V = 0.03$ W/m · K; $R_1 = 6$, $R_2 = 9.5$, and $R_3 = 12$ cm.

heat source is changed significantly while the temperature of the cold source keeps almost unchanged. Figures 3(a)–3(c) show the measured temperatures at the three centers, which are almost constant as predicted by the theory. The constant value is a little lower than the phase-transition temperature (297.2 K) due to the dissipation of heat to the environment. Meanwhile, the temperature distributions of the device without the SMA are also presented in Figs. 3(d)–3(f) for comparison. In this case, the temperatures within the central areas vary significantly [Figs. 3(d)–3(f)].

Apply the energy-free thermostat concept to design a new thermal cloak.—To make our thermostat concept more useful, we try applying it to thermal cloaking [11–18]. As a result, we shall achieve an improved thermal cloak whose central region serves as an ideal thermal environment with a constant temperature even though the environmental temperature gradient changes significantly. This feature makes the improved thermal cloak distinctly different from the existing thermal cloaks (whose central temperatures vary evidently as environmental temperature gradients change significantly) [11–18].

A thermal cloak helps to steer heat flow around an object without the need of disturbing the temperature distribution outside the object, and it has two basic characteristics: an undisturbed temperature field outside and a uniform temperature field inside [11–18]. To design our improved thermal cloak, we resort to the structure of bilayer thermal cloak [18] by using four types of materials; see Fig. 4(a) which shows regions I-VI for the new device in a background with thermal conductivity κ_0.

Regions I-IV have a height of $2R_1$, and they are occupied by the four types of materials, whose thermal conductivities are, respectively, given by

$$\kappa_I = \kappa_0 - \frac{(\kappa_0 - \kappa_i)}{1 + e^{T-T_C}}, \quad \kappa_{II} = \kappa_0 - \frac{(\kappa_0 - \kappa_i)e^{T-T_C}}{1 + e^{T-T_C}},$$
$$\kappa_{III} = \kappa_0 + \frac{(\kappa_e - \kappa_0)}{1 + e^{T-T_C}}, \quad \kappa_{IV} = \kappa_0 + \frac{(\kappa_e - \kappa_0)e^{T-T_C}}{1 + e^{T-T_C}}. \quad (5)$$

These conductivities may be manufactured by utilizing the multistep approximation method as employed in the experimental design [Fig. 2(c)]. On the other hand, regions V and VI in Fig. 4(a) are occupied by two common materials with conductivities

$$\kappa_V \to 0 \quad \text{and} \quad \kappa_{VI} = \kappa_0(R_3^2 + R_2^2)/(R_3^2 - R_2^2), \quad (6)$$

according to the requirement of bilayer thermal cloaks [18]. The simulation results in Figs. 4(b)–4(d) show that as the temperature of the heat source is increased from 323.2, to 338.2, and then to 353.2 K, the improved thermal cloak is able to energy-freely maintain an approximately constant temperature inside it indeed; see 293.5, 294.0, and 294.7 K as indicated in Figs. 4(b)–4(d). We obtain this conclusion by comparing the "293.5, 294.0, and 294.7 K" with their counterpart values of the common cloaking (namely, "298.2, 305.7, and 313.2 K," which are calculated by averaging the two temperatures of the cold and hot sources when the cloak is located in the center between the two sources).

Conclusions.— We have established a temperature-trapping theory for asymmetric phase-transition materials

with thermally responsive thermal conductivities, and introduced a concept of an energy-free thermostat. The thermostat is capable of self-maintaining a desired constant temperature without energy consumption even though the environmental temperature gradient varies in a large range. By using a multistep approximation method, we have experimentally fabricated a prototype device. In the experiment, we employed homogenous isotropic materials and SMAs (shape memory alloys), which are commercially available. Since no heat engine or temperature sensor is used, the device is lightweight and can be used as components of larger facilities or buildings without interference. For instance, inspired by this concept, we have theoretically designed and showed a different type of thermal cloak that has a constant temperature inside its central region in spite of changing ambient temperature gradients, which is in sharp contrast to all the existing thermal cloaks [11–18]. Our results have relevance to energy-saving temperature preservation, and they are indicative of a great freedom in extensibility, e.g., for controlling the flow of heat with zero-energy consumption and for designing new metamaterials with temperature-responsive or field-responsive parameters in many disciplines such as thermotics, optics, electromagnetics, acoustics, mechanics, electrics, and magnetism.

We thank Professor Hong Zhao, Dr. Yilong Han, and Dr. Lei Xu for fruitful discussions. We acknowledge financial support by the Science and Technology Commission of Shanghai Municipality under Grant No. 16ZR1445100.

X. S. and Y. L. contributed equally to this work.

*jphuang@fudan.edu.cn

[1] S. Chu and A. Majumdar, Opportunities and challenges for a sustainable energy future, Nature (London) **488**, 294 (2012).

[2] M. Maldovan, Phonon wave interference and thermal bandgap materials, Nat. Mater. **14**, 667 (2015).

[3] Y. Hu, L. Zeng, A. J. Minnich, M. S. Dresselhaus, and G. Chen, Spectral mapping of thermal conductivity through nanoscale ballistic transport, Nat. Nanotechnol. **10**, 701 (2015).

[4] L. E. Bell, Cooling, heating, generating power, and recovering waste heat with thermoelectric systems, Science **321**, 1457 (2008).

[5] K. Biswas, J. He, I. D. Blum, C.-I. Wu, T. P. Hogan, D. N. Seidman, V. P. Dravid, and M. G. Kanatzidis, High-performance bulk thermoelectrics with all-scale hierarchical architectures, Nature (London) **489**, 414 (2012).

[6] L. D. Zhao, S.-H. Lo, Y. Zhang, H. Sun, G. Tan, C. Uher, C. Wolverton, V. P. Dravid, and M. G. Kanatzidis, Ultralow thermal conductivity and high thermoelectric figure of merit in SnSe crystals, Nature (London) **508**, 373 (2014).

[7] B. Li, L. Wang, and G. Casati, Thermal Diode: Rectification of Heat Flux, Phys. Rev. Lett. **93**, 184301 (2004).

[8] C. W. Chang, D. Okawa, A. Majumdar, and A. Zettl, Solid-state thermal rectifier, Science **314**, 1121 (2006).

[9] M. J. Martínez-Pérez, A. Fornieri, and F. Giazotto, Rectification of electronic heat current by a hybrid thermal diode, Nat. Nanotechnol. **10**, 303 (2015).

[10] C. J. Glassbrenner and G. A. Slack, Thermal conductivity of silicon and germanium from 3 K to the melting point, Phys. Rev. **134**, A1058 (1964).

[11] Y. Li, X. Shen, Z. Wu, J. Huang, Y. Chen, Y. Ni, and J. Huang, Temperature-Dependent Transformation Thermotics: From Switchable Thermal Cloaks to Macroscopic Thermal Diodes, Phys. Rev. Lett. **115**, 195503 (2015).

[12] C. Z. Fan, Y. Gao, and J. P. Huang, Shaped graded materials with an apparent negative thermal conductivity, Appl. Phys. Lett. **92**, 251907 (2008).

[13] S. Narayana and Y. Sato, Heat Flux Manipulation with Engineered Thermal Materials, Phys. Rev. Lett. **108**, 214303 (2012).

[14] M. Maldovan, Sound and heat revolutions in phononics, Nature (London) **503**, 209 (2013).

[15] R. Schittny, M. Kadic, S. Guenneau, and M. Wegener, Experiments on Transformation Thermodynamics: Molding the Flow of Heat, Phys. Rev. Lett. **110**, 195901 (2013).

[16] Y. Ma, Y. Liu, M. Raza, Y. Wang, and S. He, Experimental Demonstration of a Multiphysics Cloak: Manipulating Heat Flux and Electric Current Simultaneously, Phys. Rev. Lett. **113**, 205501 (2014).

[17] H. Xu, X. Shi, F. Gao, H. Sun, and B. Zhang, Ultrathin Three-Dimensional Thermal Cloak, Phys. Rev. Lett. **112**, 054301 (2014).

[18] T. Han, X. Bai, D. Gao, J. T. L. Thong, B. Li, and C.-W. Qiu, Experimental Demonstration of a Bilayer Thermal Cloak, Phys. Rev. Lett. **112**, 054302 (2014).

[19] U. Leonhardt, Optical conformal mapping, Science **312**, 1777 (2006).

[20] J. B. Pendry, D. Schurig, and D. R. Smith, Controlling electromagnetic fields, Science **312**, 1780 (2006).

[21] A. A. High, R. C. Devlin, A. Dibos, M. Polking, D. S. Wild, J. Perczel, N. P. de Leon, M. D. Lukin, and H. Park, Visible-frequency hyperbolic metasurface, Nature (London) **522**, 192 (2015).

[22] N. Kaina, F. Lemoult, M. Fink, and G. Lerosey, Negative refractive index and acoustic superlens from multiple scattering in single negative metamaterials, Nature (London) **525**, 77 (2015).

[23] R. Zheng, J. Gao, J. Wang, and G. Chen, Reversible temperature regulation of electrical and thermal conductivity using liquid-solid phase transitions, Nat. Commun. **2**, 289 (2011).

[24] D.-W. Oh, C. Ko, S. Ramanathan, and D. G. Cahill, Thermal conductivity and dynamic heat capacity across the metal-insulator transition in thin film VO2, Appl. Phys. Lett. **96**, 151906 (2010).

[25] K. S. Siegert, F. R. L. Lange, E. R. Sittner, H. Volker, C. Schlockermann, T. Siegrist, and M. Wuttig, Impact of vacancy ordering on thermal transport in crystalline phase-change materials, Rep. Prog. Phys. **78**, 013001 (2015).

[26] J. P. Huang and K. W. Yu, Enhanced nonlinear optical responses of materials: Composite effects, Phys. Rep. **431**, 87 (2006).

[27] C. Chluba, W. Ge, R. L. de Miranda, J. Strobel, L. Kienle, E. Quandt, and M. Wuttig, Ultralow-fatigue shape memory alloy films, Science **348**, 1004 (2015).

[28] D. Dye, Shape memory alloys: Towards practical actuators, Nat. Mater. **14**, 760 (2015).